



## Compensating steel web-opened beams for the loss in cyclic shear capacity by longitudinal stiffeners

Yasmin Ali<sup>1</sup>, Ahmed Elgammal<sup>2</sup>

<sup>1,2</sup>Civil Engineering Department, Faculty of Engineering, Delta University for Science and Technology, Gamasa, Egypt

Correspondence: [Yasmin Ali]; [Delta University for Science and Technology, International Coastal Road, Gamasa, Egypt]; Tel [+20502770140]; Email: [yasmin.ali@deltauniv.edu.eg](mailto:yasmin.ali@deltauniv.edu.eg)

### ABSTRACT

In construction practices nowadays, web openings are provided in steel beams to allow room for services, such as pipes and air ducts, to pass through them. However, these web openings have been proved to cause a loss in the shear capacity. Accordingly, in this research a high-performance technique is adopted to compensate web-opened beams for the loss in their shear capacity; particularly when they are subjected to cyclic loading. That technique represents in the installation of additional longitudinal stiffeners in the panel adjacent to the one containing the opening; thus, mitigating shear buckling in that panel and increasing the cyclic shear capacity. For this purpose, a 3-D finite element (FE) model, using Ansys Workbench, was utilized to investigate one solid web beam in addition to eight web-opened beams. Each of the failure mode, cyclic shear capacity and deflection of the specimens were comprehensively investigated. The results indicated that the installation of additional longitudinal stiffeners is an efficient solution to overcome the loss in cyclic shear capacity of web-opened beams, especially in the case of relatively small openings. They even raised the cyclic shear capacity to more than that of the solid web specimen. In the case of large openings, longitudinal stiffeners managed also to improve the cyclic shear capacity despite not reaching that of the solid web specimen.

**Keywords:** Cantilever; Cyclic loading; Web opening; Longitudinal stiffener; Shear strength.

### 1. Introduction

I-section beams, and girders, are widely used nowadays in different steel structures. The reason for adopting such cross-section is attributed to its consistency with typical normal stress distribution. In other words, it has large width near the upper and lower fibers which are subjected to the extreme normal stresses. Moreover, the rest of the cross-section has a reduced width since the normal stresses keep decreasing till reaching the neutral axis. Generally, a typical I-section consists of two parallel flanges connected with a flat web that is equipped with a set of transverse stiffeners. The flanges are mainly responsible to resist the axial loads resulting from the acting bending moment. On the other hand, the web responsibility is to resist the acting shear forces, whereas the stiffeners are responsible for mitigating the shear buckling that the web encounters. Thus, it can be inferred that the web is the main factor in determining the shear strength of I-section beams and girders; any sort of deficiency in the web could lead to a loss in the overall shear capacity. By drawing attention to the offshore platforms and bridges, I-section beams and girders in them are usually provided with web openings to leave sufficient room for cabling, services, maintenance and inspection [1], [2]. These openings may take the form of square, rectangle, circle, elongated circle, hexagon, or even octagon [3]. Aspect ratio of the openings usually ranges from 1 to 3, while their depth approximately represents 50 [3] to 60% [4] of the beam depth. Existence of these openings in the web results in the reduction of the web area, which is responsible for resisting shear forces as mentioned above. Therefore, web-opened beams suffer from shear capacity loss compared to those with solid webs [5]. Narayanan and Der Avanessian [6] attributed this issue to the fact that the reduction of the width of membrane stresses that are developed all over the diagonal tension field, which contributes in carrying the load in the post-critical stage, is dependent on the largest dimension of the opening. This reflects the higher web plastic shear resistance of solid webs compared to opened webs as shown in Eq. (1) [2], [7].

$$V_{pl,w} = \begin{cases} \frac{f_{yw}}{\sqrt{3}} h_w t_w \text{ (solid web)} \\ \frac{f_{yw}}{\sqrt{3}} (h_w - d_0) t_w \text{ (opened web)} \end{cases} \quad (1)$$

where  $V_{pl,w}$  is the plastic shear resistance of the web,  $f_{yw}$  is the tensile yield stress of the web material,  $h_w$  is the web clear height,  $t_w$  is the web thickness, and  $d_0$  is the depth of the opening.

Web-opened beams were extensively studied in literature, whether experimentally or theoretically. However, the factor these studies had in common was that all the studied beams were subjected to monotonic loading. For instance, Thevendran and Shanmugan [8] conducted both experimental and numerical studies on steel beams with circular as well as rectangular openings. Chung and Lawson [9] proposed a design method for composite beams with large web openings in addition to presenting design rules for circular openings. Moreover, Chung et al. [10] suggested an empirical design method that is valid for steel beams having openings of distinctive shapes and sizes on the basis of generalized moment-shear interaction curves. Mohebkah [11] investigated the effect of slenderness on the moment-gradient factor of a special type of web-opened beams (called castellated beams). He, as well, developed alternative equations for the moment-gradient factor. Tsavdaridic and D'Mello [12] introduced novel non-standard opening shapes that can enhance the overall structural performance of web-opened beams. Additionally, Sweedan [13] proposed a simplified approach to accurately predict the moment modification factor for web-opened beams. Regarding the load-carrying capacity, Erdal and Saka [14] investigated it for steel web-opened beams. They also demonstrated that web-opened beams may either fail due to web-post buckling, web shear buckling or Vierendeel bending. Panedpojaman and Thepchatri [15] introduced a method to predict the deflection of web-opened beams. In addition, Boissonnade et al. [16] developed a design method for the lateral torsional buckling of web-opened beams. More recently, the experimental and numerical results of Morkhade et al. [17]–[21] proved that both of the load carrying capacity and stiffness are inversely proportional to the opening area. They also illustrated that rectangular web openings suffer from high stress concentrations near the corners. Alternatively, several techniques were proposed, in literature, to limit the loss in shear capacity of web-opened beams and girders as follows:

- a) Curving the corners of rectangular/square web openings to mitigate stress concentrations [4].
- b) Utilizing reinforcements around the opening to compensate for the reduction in the shear strength [1], [4].
- c) Positioning small openings on the far ends of the compression diagonal [6].
- d) Replacing flat flanges with tubular ones since their vertical segments contribute in resisting shear forces [2], [22], [23].

In light of this, the current research aims to numerically study the cyclic shear capacity of web-opened beams and to compensate the loss in shear strength by a novel technique. This technique represents in equipping the beam with additional longitudinal stiffeners in the solid panels. That technique is inspired by the numerical work of Elgammal [24]. Although the previous studies were involved with link beams in eccentrically braced frames, an important remark could be observed; a cyclically loaded I-section beam can have its shear strength improved by equipping it with longitudinal stiffeners. Thereupon, this technique is chosen to be investigated herein. The reason for studying web-opened beams subjected to cyclic loading rather than monotonic loading is because of the lack of research concerned with this issue.

## 2. Numerical Modeling and validation

### 2.1. General

To simulate the behavior of steel beams with square web openings, 3-D finite element (FE) models were developed using Ansys Workbench (2020 R1) [25]. The current numerical study includes the analysis of a total number of nine specimens made of S275 steel [26], loaded as cantilever beams, as described in Table 1. Note that,  $L$  is the span of the cantilever,  $B_f$  and  $t_f$  are the flange width and thickness, respectively,  $h_w$  and  $t_w$  are the web clear height and thickness, respectively,  $t_s$  is the stiffener thickness,  $a$  is the stiffener spacing, and  $d_0$  is the depth of the square opening. Moreover, “T” denotes a beam with transverse stiffeners, whereas “T+L” denotes a beam with both transverse and longitudinal stiffeners, as shown in Fig. 1. The first specimen is a control specimen which has a solid web without any sort of openings. The other specimens are all provided with square openings in the center of the first web panel adjacent to the fixed support. This is the critical web panel since it is subjected to the highest shear force as well as bending moment. The opening depth to web clear height ratio ( $d_0/h_w$ ) that ranges from 0.1 to 0.7. Accordingly, an evaluation of the effect of several openings’ depth could be carried out. The web-opened specimens may either be equipped with conventional transverse stiffeners or the combination of transverse

stiffeners and longitudinal stiffeners. These longitudinal stiffeners are particularly placed in the solid web panels that are adjacent to the opened panels. All of the specimens in the current study were designed due to web shear buckling; they all have slender webs and compact flanges according to [26]. It is worth to mention that the specimens were labelled in such a way that their properties could be identified. Each label begins with a letter that denotes the status of the web; “S” denotes a solid web, whereas “O” denotes an opened web. It is then followed by a number representing  $d_0/h_w$  ratio. Of course, the control specimen (first specimen) had  $d_0/h_w$  equal to zero since it did not include any web openings. Eventually, the label ends with one/two letters denoting the configuration of the stiffeners within the specimen; “T” represents a specimen with transverse stiffeners only, whereas “TL” represents a specimen with both transverse and longitudinal stiffeners.

Table 1. Details of the specimens.

Specimen	$L$ (mm)	$B_f$ (mm)	$t_f$ (mm)	$h_w$ (mm)	$t_w$ (mm)	$t_s$ (mm)	$\frac{a}{h_w}$	$\frac{d_0}{h_w}$	Stiffener
S-0-T	1000	180	10	500	3	10	1.0	—	T
O-0.1-T	1000	180	10	500	3	10	1.0	0.10	T
O-0.1-TL	1000	180	10	500	3	10	1.0	0.10	T+L
O-0.3-T	1000	180	10	500	3	10	1.0	0.30	T
O-0.3-TL	1000	180	10	500	3	10	1.0	0.30	T+L
O-0.5-T	1000	180	10	500	3	10	1.0	0.50	T
O-0.5-TL	1000	180	10	500	3	10	1.0	0.50	T+L
O-0.7-T	1000	180	10	500	3	10	1.0	0.70	T
O-0.7-TL	1000	180	10	500	3	10	1.0	0.70	T+L

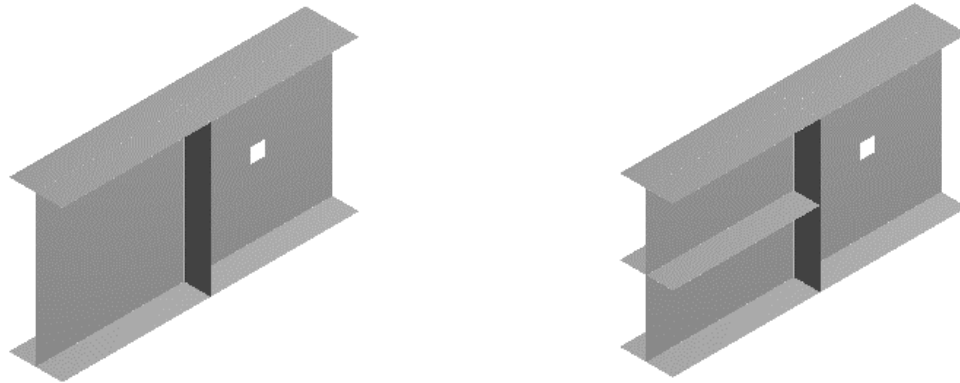


Fig. 1. Typical specimens with transverse stiffeners only (left), and both transverse and longitudinal stiffeners (right).

## 2.2. Details of the finite element model

The four-node linear SHELL181 element [27], in Ansys [25] element library, was utilized in the current FE model of the specimens herein. It was indicated in literature [28], [29] that the web clear height should be divided into 16 to 30 elements in order to accurately predict the shear behavior of girders. However, a mesh sensitivity analysis (convergence test) was carried out on S-0-T specimen to obtain the optimum mesh size. The web clear height, in that analysis, was divided into four different numbers: namely, 15, 20, 25, and 30. Fig. 2 shows the variation of the ultimate shear strength with the change of web height divisions. It is obvious that increasing web height divisions causes insignificant change in the ultimate shear strength. At the same time, a sharp increase in the computation time is found to accompany that increment in web height divisions. For instance, increasing web height divisions by 33% (from 15 to 20) caused the ultimate shear strength to drop by only 1%; on the other hand, it caused the computation time to severely increase by 86%. The same remark is noticed for the remaining web height divisions. On this basis, dividing the web height into only 15 elements was sufficient herein to obtain reasonable results.

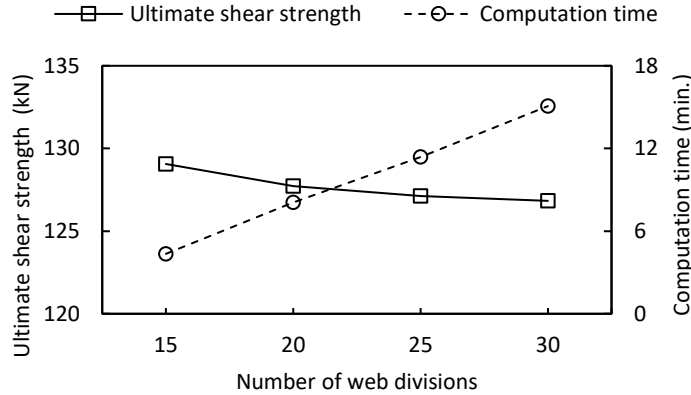


Fig. 2. Analysis of mesh sensitivity for S-0-T.

The beam was applied with controlled vertical displacements, following the cyclic loading protocol shown in Fig. 3, at the whole cross-section of the free end. This cyclic loading protocol is scaled down from the original loading protocol of AISC 341-16 [30]. The reason for such scale down is that the original loading protocol of [30] was mainly developed for beam-column joints in moment-resisting frames; so, it is not suitable for the nature of the cantilever beams in its original form since it requires very high displacements to be applied to the extent that the beams could not survive. The controlling parameter in the adopted cyclic loading protocol is the drift angle which can be expressed as the ratio of the vertical displacement at the free end to the span length of the beam. The other end of the beam was kept completely fixed.

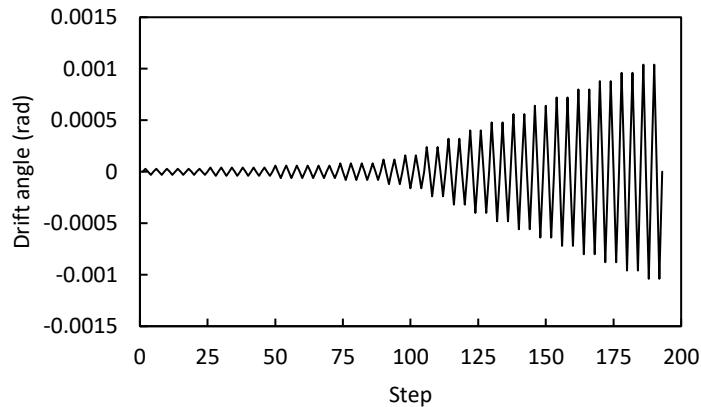


Fig. 3. The applied cyclic loading protocol.

According to the experimental and numerical work of Krolo et al. [31], the cyclic behavior of S275 steel is different from its monotonic behavior. This is because most cyclically loaded metallic alloys exhibit both isotropic and kinematic hardening not just one of them as in monotonic loading cases. Therefore, the above-mentioned researchers proposed that particular steel to be modeled in numerical simulations based on Chaboche combined hardening model [32]. In this hardening model, the kinematic hardening ( $\alpha$ ) is expressed as follows [32]:

$$\alpha = \sum_{i=1}^n \frac{C_i}{\gamma_i} (1 - e^{-\gamma_i \epsilon^{pl}}) + \alpha_i^0 e^{-\gamma_i \epsilon^{pl}} \quad (2)$$

$C_i$  and  $\gamma_i$  are the kinematic hardening constants of the  $i$ th kinematic hardening,  $\alpha_i^0$  is the initial value of the  $i$ th kinematic hardening, and  $\epsilon^{pl}$  is the plastic strain. With regard to the isotropic hardening module, Chaboche [32] recommended to calculate it according to Voce law [33] as follows:

$$\sigma^0 = \sigma|_0 + Q_\infty(1 - e^{-b\varepsilon^p}) \quad (3)$$

$\sigma^0$  is the isotropic hardening yield surface,  $\sigma|_0$  is the initial yield stress of the material,  $Q_\infty$  and  $b$  are the isotropic hardening parameters. To properly model the cyclic behavior of S275 steel, Krolo et al. [31] suggested all the parameters mentioned before to be taken as listed in Table 2. Young's modulus and Poisson's ratio were also taken, according to [31], as 207000 MPa and 0.3, respectively.

Table 2. Chaboche combined hardening parameters for S275 steel [31].

Kinematic hardening				Isotropic hardening				
$C_1$	$\gamma_1$	$C_2$	$\gamma_2$	$C_3$	$\gamma_3$	$\sigma _0$	$Q_\infty$	$b$
13921	765	4240	52	1573	14	285	25.6	4.4

Note: the unit of  $C_i$  and  $\sigma|_0$  is MPa.

In the current FE models, geometric imperfections were taken into account through conducting first an Eigenvalue buckling analysis to determine the first buckling mode. Then, that buckling mode was imported into the perfect geometry of the beam in the step of nonlinear load-displacement analysis. The value of the geometric imperfections, in the current research were taken as  $h_w/100$  as per [34]. In contrast, residual stresses were neglected, as recommended by Dong and Sause [35], since the unbraced length of the current specimens is less than 20 m.

### 2.3. Validation of the finite element model

To check the accuracy of the current FE model, it should be checked against existing experimental tests. Indeed, the authors conducted several verification studies on structural elements subjected to cyclic loading; refer to [24], [36]–[39]. However, two specimens, labelled as specimen 1 and specimen 4, of the experimental tests of Hjelmstad and Popov [40] were used to validate the current FE model. Hjelmstad and Popov [40] experimentally tested fifteen link beams to study their cyclic shear performance. Note that link beams constitute the main component of the earthquake resistant system known as the eccentrically braced frame. Only the prementioned specimens were chosen for the verification study since they were the only ones that had their hysteretic response and failure modes presented. The cross-section of both specimens was W18×40. They also shared the same span length of 711.2 mm. The material of construction was ASTM A36 and its Chaboche combined hardening parameters were taken following the work in [41]. The only difference between the specimens was the stiffener configuration. Specimen 1 did not include stiffeners, while specimen 4 included three stiffeners, at equal spacings, of a 9.53 mm thickness. The displacement-controlled cyclic loading protocol consisted of a single cycle of 12.7 mm, then followed by dual cycles of 25.4, 38.1, 50.8 mm, etc. The boundary conditions were taken according to the work in [24]. The hysteretic curves of shear force and rotation angle obtained from the current FE model are plotted along with those of the experimental test in Fig. 4. It is evident that an adequate agreement is achieved between the experimental and the results of the current FE model. For instance, the ratio of the ultimate shear strength in the experimental test to the FE results is 1.13 and 1.1 for specimen 1 and specimen 4, respectively. In addition, the failure modes of the specimens, shown in Fig. 5, attest that the current FE model can precisely predict the deformed shapes of the specimens at the failure stage.

## 3. Results and discussion

As mentioned earlier, the only difference between the nine specimens, under consideration, is the opening depth and stiffener configuration. Thus, all nine specimens share the same plastic moment resistance withal different plastic shear resistance. Based on the FE results, the maximum cyclic shear capacity was obtained and reported in Table 3. In the following, a discussion on the FE results is presented.

### 3.1. Mode of failure

Steel beams could develop several modes of failure. Nevertheless, the current specimens were properly designed to fail due to web shear buckling; other modes of failure were prevented. For instance, local buckling of the flanges was disallowed through employing compact flanges, while local buckling and crippling of the web were also prevented through applying the load evenly at the free end in addition to the installation of sufficient stiffeners.

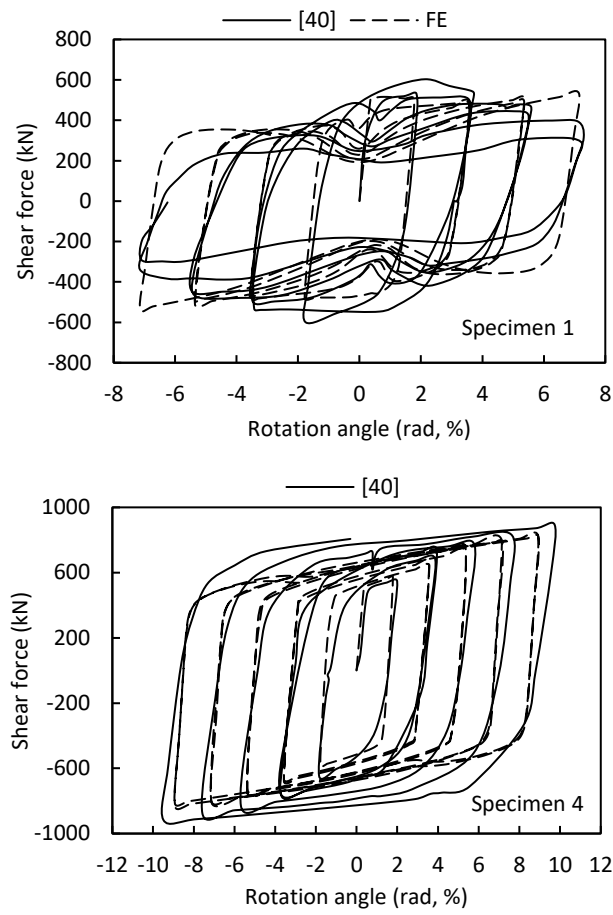


Fig. 4. Hysteretic curves of the specimens.

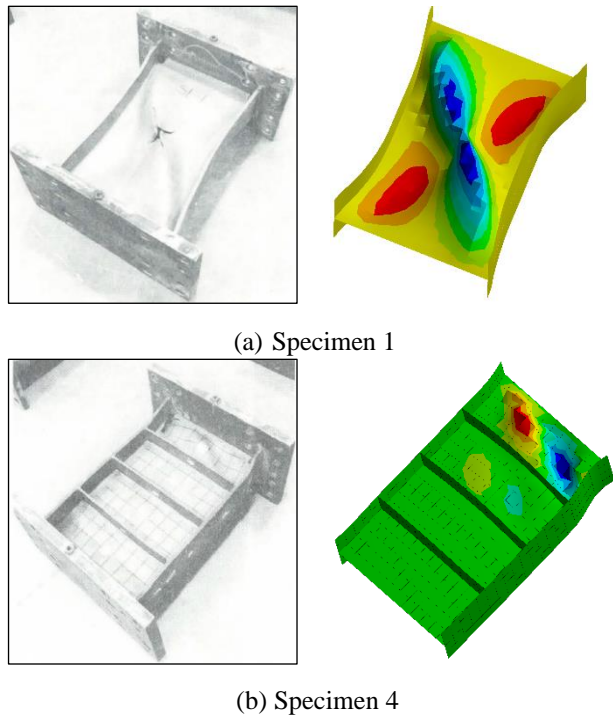


Fig. 5. Failure modes obtained from the experimental test (left) and the FE simulation (right).

All the specimens failed due to web shear buckling. It was also noticed that no shear-based plastic hinges were developed in the flanges, as shown in Fig. 6. In S-0-T, web shear buckling firstly propagated near the load location at the free end, as shown in Fig. 6(a); that figure depicts the deformed shape and von-Mises stress distribution at the step in which the beam reaches its ultimate shear carrying capacity. In addition, no obvious sign of web shear buckling at the web panel near the support was observed. In contrast, existence of web openings in O-0.1-T and O-0.3-T caused the regions of the web near the opening to also buckle out-of-plane. Nonetheless, most of the web shear buckling occurred near the free end in the same manner as S-0-T. Thereupon, equipping the outer web panel with longitudinal stiffener, in O-0.1-TL and O-0.3-TL, had a vital effect on mitigating web shear buckling in that panel to the extent that the latter was nearly eliminated. Bearing in mind that web shear buckling was still found around the opening. However, it was mitigated either. O-0.5-T and O-0.7-T, containing larger web openings, had a different scheme of web shear buckling. Due to the large dimensions of the openings, they highly altered the location of the maximum out-of-plane displacement. To be specific, web shear buckling was mainly concentrated around the edges of the openings. On the opposite, the outer web panel did not show any web shear buckling. Therefore, equipping those specimens with longitudinal stiffeners (O-0.5-TL and O-0.7-TL) did not change the distribution of web shear buckling. So, it can be demonstrated that small web openings ( $d_0/h_w \leq 0.3$ ), in web-opened beams, do not much influence the web shear buckling with respect to that of solid-web beams. On the contrary, large web openings ( $d_0/h_w > 0.3$ ) weaken the web panel in which they are included; thus, causing most of the web shear buckling to develop around them before any significant web shear buckling takes place in other panels.

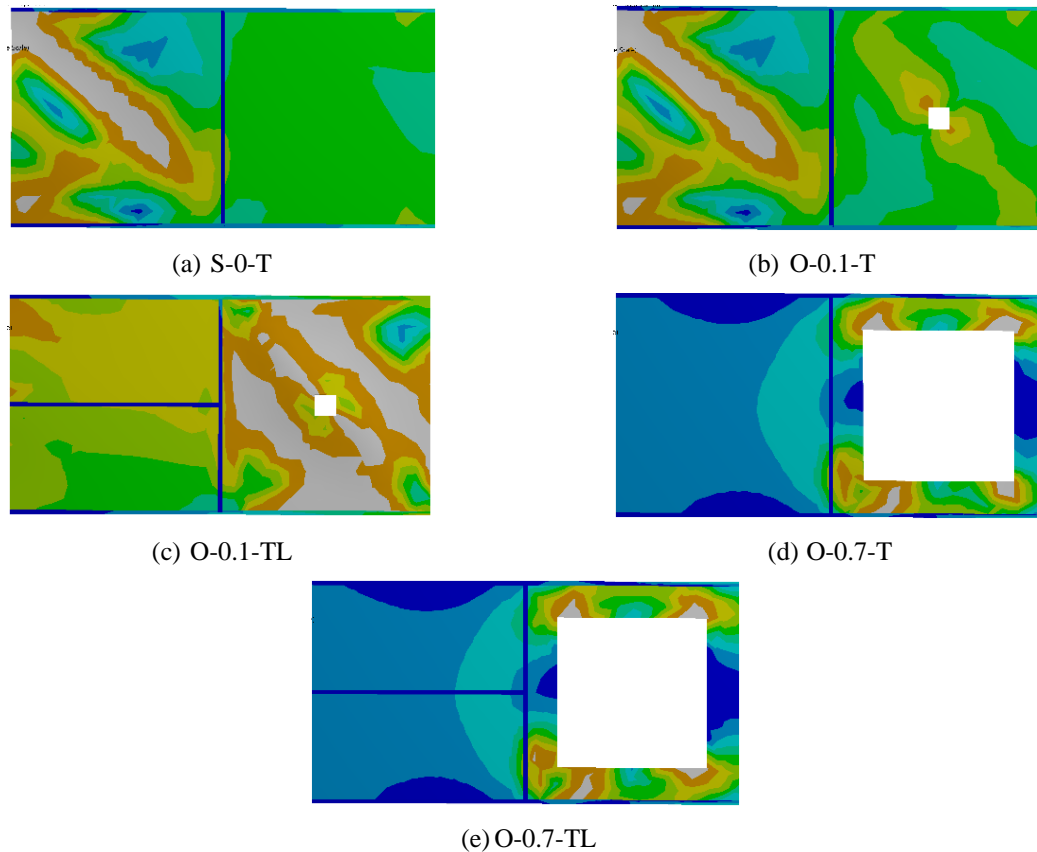


Fig. 6. A plot of the deformed shape and von-Mises stress distribution at the ultimate cyclic shear capacity (grey contours represent the regions that exceeded the yield stress).

### 3.2. Effect of relative web opening size ( $d_0/h_w$ ) on the cyclic shear capacity ( $V_{FE}$ )

Fig. 7 depicts the cyclic shear capacity ( $V_{FE}$ ) of the control specimen (S-0-T) as well as the transversely stiffened specimens; specimens with both transverse and longitudinal stiffeners were dismissed herein. It is seen that small web openings that represent 10% of the web clear height do not significantly reduce  $V_{FE}$ . Thus, the beams provided with them did not have any loss in the cyclic shear capacity compared to the control specimen. This does not apply

to larger web openings as they noticeably affect  $V_{FE}$ . For example, web openings representing 30, 50, and 70% of the web clear height caused  $V_{FE}$  to drop by 12, 38, and 51%, respectively, compared to the control specimen. Therefore, web openings are proved herein to have a severe effect on the cyclic shear capacity of cantilever beams, especially the relatively large ones.

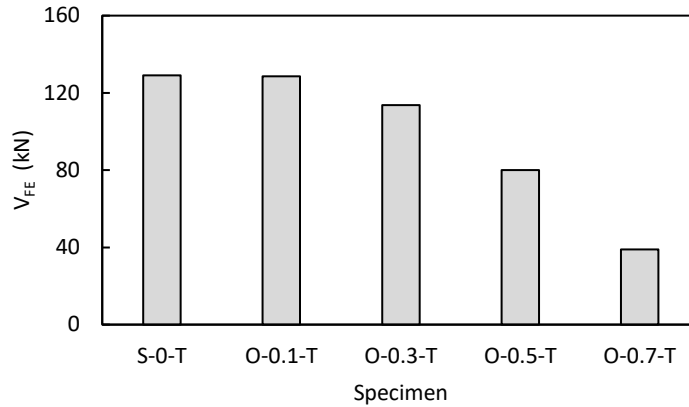


Fig. 7.  $V_{FE}$  for the control specimen and web-opened specimens.

### 3.2. Effect of stiffener configuration on the cyclic shear capacity ( $V_{FE}$ )

In Fig. 8,  $V_{FE}$  of specimens with transverse stiffeners (denoted by T) and specimens with both transverse and longitudinal stiffeners (denoted by T+L) for each relative web opening size is illustrated. As mentioned before, all web-opened specimens, except the one with  $d_0/h_w = 0.1$ , have lower  $V_{FE}$  than that of the control specimen ( $V_C = 129.1$  kN). Moreover, it can be observed that equipping the specimens with additional longitudinal stiffeners did not only enhance their cyclic shear capacity, but it also caused it to exceed the control specimen in some cases. This particularly took place in the specimens having openings with  $d_0/h_w$  up to 0.3. In details, in the case of  $d_0/h_w = 0.1$  and 0.3, the longitudinal stiffeners managed to improve  $V_{FE}$  by 38 and 34%, respectively, compared to the specimens with transverse stiffeners only. Not just that, the specimens with longitudinal and transverse stiffeners having  $d_0/h_w = 0.1$  and 0.3 had  $V_{FE}$  that exceed the control specimen by 38 and 18%, respectively. So, longitudinal stiffeners managed to compensate the web-opened beams for the loss in their cyclic shear capacity. Furthermore, the installation of additional longitudinal stiffeners in the specimens with larger web openings ( $d_0/h_w = 0.5$  and 0.7) improved the cyclic shear capacity compared to those with transverse stiffeners only. However, this time longitudinal stiffeners did not enable the web-opened beams to reach higher  $V_{FE}$  than the control specimen. The interpretation of this is that the specimens with small  $d_0/h_w$  (up to 0.3) had significant shear buckling in the outer panel, as illustrated in Fig. 6. Accordingly, equipping that panel with longitudinal stiffener noticeably mitigated that shear buckling and thus enhanced the overall carrying capacity. In the case of large opening sizes ( $d_0/h_w > 0.3$ ), minor shear buckling took place in the outer panel. Consequently, equipping that panel with longitudinal stiffener insignificantly limited the out-of-plane displacement. So, the enhancement resulting from the longitudinal stiffeners was meaningless as in the case smaller web openings.

### 3.3. Additional deflection

It was reported in literature that the existence of web openings affect the bending moment and shear force distribution through the cross-section height which causes additional deflection compared to solid web beams; see [9], [42] for more details. Thereby, a web-opened beam will suffer from higher vertical displacement, at the free end, compared to the similar beam with a solid web. The free end vertical displacement corresponding to  $V_{FE}$ , as a consequence, is normalized through dividing it by the same value for the control specimen having solid web (S-0-T) and shown in Fig. 9. It is detected that all web-opened specimens have normalized vertical displacement exceeding unity. In other words, they were all subjected to higher deflection compared to the solid web specimen. Apparently, this is consistent with the previous studies mentioned above. In the case of  $d_0/h_w = 0.1$ , the additional deflection surpassed that of the control specimen by only 5%, which is not significant. Nonetheless, larger  $d_0/h_w$  caused a severe increase in the additional deflection; for  $d_0/h_w$  ranging from 0.3 to 0.7, the average increase in



the additional deflection was 46%. Arguably, additional deflection is relatively proportional to the dimensions of the square opening. Regarding the longitudinal stiffeners, their presence resulted in a minor increase in the additional deflection compared to the corresponding specimens with transverse stiffeners only. For instance, the specimens with longitudinal stiffeners have higher additional deflection than those with transverse stiffeners only by the average of 2%. This is attributed to the fact that the specimens with longitudinal and transverse stiffeners can bear higher loads compared to the others with transverse stiffeners only. That extra load bearing surely caused the beams to exhibit higher deflection. However, that increase, estimated of averagely 2%, is insignificant and thus negligible.

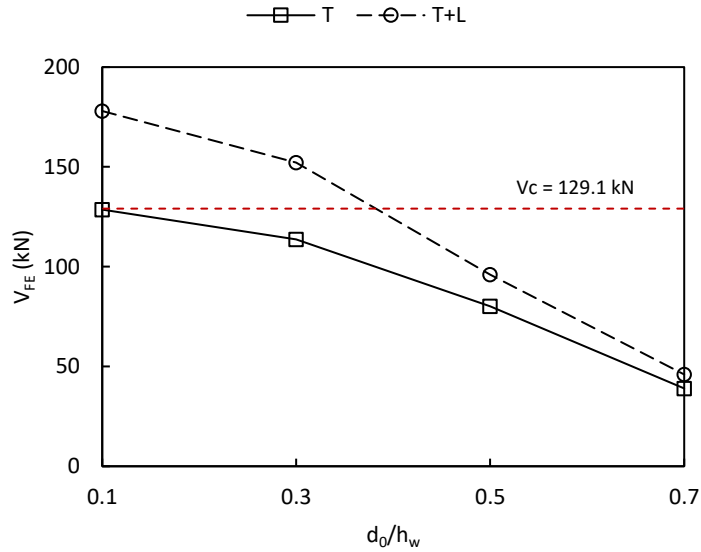


Fig. 8. The applied cyclic loading protocol.

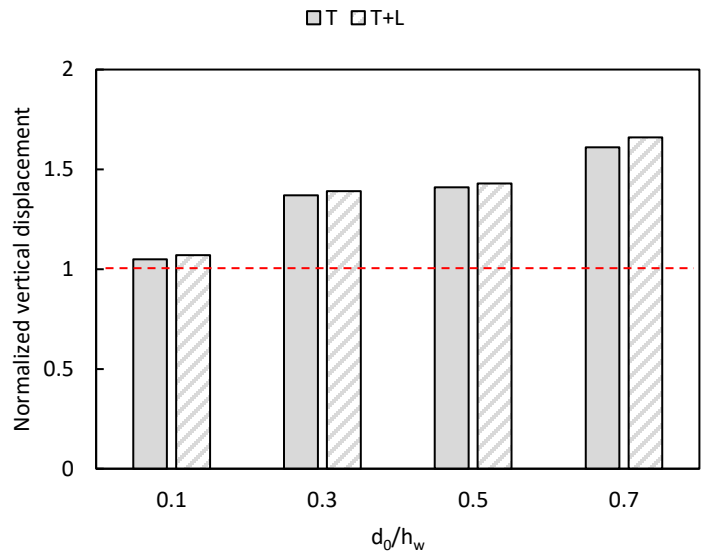


Fig. 9. Normalized free end vertical displacement of the web-opened specimens.

**4. Conclusions**

A high-performance technique is proposed herein, in this research, to compensate steel beams for the loss in their cyclic shear capacity corresponding to the existence of openings in their webs. That technique mainly depends on

equipping the web panel adjacent to the opened one with longitudinal stiffeners; thus, shear buckling in that panel could be mitigated resulting in an increase in the cyclic shear capacity. Hence a numerical study was conducted on a solid web specimen and additional eight web-opened specimens to investigate the effect of longitudinal stiffeners on the shear strength of cantilever beams with square openings having different side lengths. On the basis of the accurately validated numerical results, several conclusions may be drawn as follows:

- a) All the, cyclically loaded, specimens in this research failed due to web shear buckling without the development of shear-based plastic hinges in the flanges of any of them. For specimens with relative opening size ( $d_0/h_w$ ) less than or equal to 0.3, most of the shear buckling was concentrated in the web panel near the free end. The specimens with  $d_0/h_w$  exceeding 0.3 were like the opposite of that; they exhibited most of their shear buckling around the opening. So, equipping the latter with additional longitudinal stiffener did not significantly mitigate web shear buckling.
- b) Small web openings having  $d_0/h_w = 0.1$  did not cause much loss in the cyclic shear capacity of the beam; it was in the order of 0.4% only. As  $d_0/h_w$  increased more, the loss in cyclic shear capacity kept increasing too. That loss may be up to 51% in the case of  $d_0/h_w = 0.7$ .
- c) Equipping additional stiffeners to the specimens with  $d_0/h_w \leq 0.3$  did not only compensated them for the loss in their cyclic shear capacity, but they also raised the load-carrying capacity to be higher than the control specimen (with solid web) by the average of 28%. So, installation of longitudinal stiffeners is a superior technique to increase the cyclic shear capacity of cantilever steel beams. Although additional longitudinal stiffeners enhanced the cyclic shear capacity of the specimens with  $d_0/h_w > 0.3$ , that enhancement did not manage to raise the cyclic shear capacity up to the solid web specimen.
- d) The existence of web openings caused higher deflection at the free end compared to the solid web specimen. Nevertheless, that additional deflection was insignificant in the case of  $d_0/h_w = 0.1$ , while highly apparent in the case of other opening sizes. Installation of longitudinal stiffeners resulted in a minor increase in that additional deflection; this increase can be neglected.

In further research studies, a wide range of specimens should be investigated. This is to obtain a general conclusion regarding the behavior of web-opened cantilever beams with longitudinal stiffeners and to derive, in addition, design formulas for that particular type of web-opened beams.

#### Disclosure

The author reports no conflicts of interest in this work. The co-author has seen and agree with the contents of the manuscript and there is no financial interest to report.

#### References

- A. El-Gammal, "Improving the Performance of Vertical Shear Links for Enhanced Seismic Energy Dissipation," M.Sc. Thesis, Tanta University, 2021.
- A. El-Gammal, S. El-Khoriby, and A. Seleemah, "Seismic response of 2-D plane framed buildings eccentrically braced with vertical shear links," 2021.
- A. M. I. Sweedan, "Elastic lateral stability of I-shaped cellular steel beams," *J. Constr. Steel Res.*, vol. 67, no. 2, pp. 151–163, 2011, doi: 10.1016/j.jcsr.2010.08.009.
- A. Mohebkah, "The moment-gradient factor in lateral-torsional buckling on inelastic castellated beams," *J. Constr. Steel Res.*, vol. 60, no. 10, pp. 1481–1494, 2004, doi: 10.1016/j.jcsr.2004.02.002.
- A. Seleemah, S. El-Khoriby, and A. Elgammal, "Seismic Response of 2-D Plane Framed Buildings Eccentrically Braced with Vertical Shear Links," *Int. J. Adv. Struct. Geotech. Eng.*, vol. 3, no. 3, pp. 1–18, 2022, doi: 10.21608/ASGE.2022.152698.1006.
- AASHTO, AASHTO LRFD Bridge Design Specifications. Washington, D.C., 2010.
- American Institute of Steel Construction, Seismic Provisions for Structural Steel Buildings: ANSI/AISC 341-16. Chicago, Illinois, 2016.
- Ansys 2020 R1, "Structural Simulation Software." SAS IP, Inc., Canonsburg (PA, USA), 2020.
- E. Voce, "A practical strain hardening function," *Metallurgia*, vol. 51, pp. 219–226, 1955, Accessed: May 03, 2022. [Online]. Available: <https://ci.nii.ac.jp/naid/10026664071/>
- EN 1993-1-1, Eurocode 3: Design of steel structures - Part 1-1: General rules and rules for buildings. Brussels: European standard, Comité Européen de Normalisation, 2005.

- F. Erdal and M. P. Saka, "Ultimate load carrying capacity of optimally designed steel cellular beams," *Journal of Constructional Steel Research*, vol. 80. Elsevier, pp. 355–368, Jan. 01, 2013. doi: 10.1016/j.jcsr.2012.10.007.
- J. Dong and R. Sause, "Flexural strength of tubular flange girders," *J. Constr. Steel Res.*, vol. 65, no. 3, pp. 622–630, 2009, doi: 10.1016/j.jcsr.2008.02.019.
- J. L. Chaboche, "Constitutive equations for cyclic plasticity and cyclic viscoplasticity," *Int. J. Plast.*, vol. 5, no. 3, pp. 247–302, 1989, doi: 10.1016/0749-6419(89)90015-6.
- K. D. Hjelmstad and E. P. Popov, "Seismic Behavior of Active Links in Eccentrically Braced Frame," Report No. UCB/EERC-83/15, Earthquake Engineering Research Center, University of California, Berkeley, CA, USA, 1983.
- K. D. Tsavdaridis and C. D'Mello, "Web buckling study of the behaviour and strength of perforated steel beams with different novel web opening shapes," *J. Constr. Steel Res.*, vol. 67, no. 10, pp. 1605–1620, 2011, doi: 10.1016/j.jcsr.2011.04.004.
- K. F. Chung and R. M. Lawson, "Simplified design of composite beams with large web openings to Eurocode 4," *J. Constr. Steel Res.*, vol. 57, no. 2, pp. 135–164, 2001, doi: 10.1016/S0143-974X(00)00011-0.
- K. F. Chung, C. H. Liu, and A. C. H. Ko, "Steel beams with large web openings of various shapes and sizes: An empirical design method using a generalised moment-shear interaction curve," *J. Constr. Steel Res.*, vol. 59, no. 9, pp. 1177–1200, 2003, doi: 10.1016/S0143-974X(03)00029-4.
- K. F. Chung, T. C. H. Liu, and A. C. H. Ko, "Investigation on viereindeel mechanism in steel beams with circular web openings," *J. Constr. Steel Res.*, vol. 57, no. 5, pp. 467–490, 2001, doi: 10.1016/S0143-974X(00)00035-3.
- M. F. Hassanein and O. F. Kharoob, "Shear strength and behavior of transversely stiffened tubular flange plate girders," *Eng. Struct.*, vol. 32, no. 9, pp. 2617–2630, 2010, doi: 10.1016/j.engstruct.2010.04.034.
- M. F. Hassanein, "Shear strength of tubular flange plate girders with square web openings," *Eng. Struct.*, vol. 58, pp. 92–104, 2014.
- M. F. Hassanein, "Tubular Flange Girders with Slender webs containing openings," *Proc. Inst. Civ. Eng. Struct. Build.*, vol. 167, no. 8, pp. 486–494, 2014, doi: 10.1680/stbu.12.00050.
- M. M. Alinia, M. Shakiba, and H. R. Habashi, "Shear failure characteristics of steel plate girders," *Thin-Walled Struct.*, vol. 47, no. 12, pp. 1498–1506, 2009, doi: 10.1016/j.tws.2009.06.002.
- N. Boissonnade, J. Nseir, M. Lo, and H. Somja, "Design of cellular beams against lateral torsional buckling," *Proc. Inst. Civ. Eng. Struct. Build.*, vol. 167, no. 7, pp. 436–444, 2014, doi: 10.1680/stbu.12.00049.
- N. C. Hagen, P. K. Larsen, and A. Aalberg, "Shear capacity of steel plate girders with large web openings, Part I: Modeling and simulations," *J. Constr. Steel Res.*, vol. 65, no. 1, pp. 142–150, 2009, doi: 10.1016/j.jcsr.2008.03.014.
- P. Krolo, D. Grandić, and Ž. Smolčić, "Experimental and Numerical Study of Mild Steel Behaviour under Cyclic Loading with Variable Strain Ranges," *Adv. Mater. Sci. Eng.*, vol. 2016, no. November, 2016, doi: 10.1155/2016/7863010.
- P. Panedpojaman and T. Thepchatri, "Finite element investigation on deflection of cellular beams with various configurations," *Int. J. Steel Struct.*, vol. 13, no. 3, pp. 487–494, 2013, doi: 10.1007/s13296-013-3008-z.
- R. Narayanan and N. G. V. Der Avanesian, "Strength of Webs with Corner Openings," *Struct. Eng. Part B R&D Q.*, vol. 62 B, no. 1, pp. 6–11, 1984, Accessed: Jan. 12, 2021. [Online]. Available: <https://trid.trb.org/view/418060>
- S. C. Lee, J. S. Davidson, and C. H. Yoo, "Shear buckling coefficients of plate girder web panels," *Comput. Struct.*, vol. 59, no. 5, pp. 789–795, Jun. 1996, doi: 10.1016/0045-7949(95)00325-8.
- S. El-Khoriby, A. Seleemah, and A. El-Gammal, "Cyclic Performance of Vertical Shear Links Made of Different Metallic Alloys," in *International Conference on Advances in Structural and Geotechnical Engineering*, 2019, p. 14.

- S. G. Morkhade and L. M. Gupta, "An experimental and parametric study on steel beams with web openings," *Int. J. Adv. Struct. Eng.*, vol. 7, no. 3, pp. 249–260, Sep. 2015, doi: 10.1007/S40091-015-0095-4/FIGURES/20.
- S. G. Morkhade and L. M. Gupta, "Analysis of steel I-beams with rectangular web openings: experimental and finite element investigation," *Eng. Struct. Technol.*, vol. 7, no. 1, pp. 13–23, Dec. 2015, doi: 10.3846/2029882x.2015.1085332.
- S. G. Morkhade and L. M. Gupta, "Experimental investigation for failure analysis of steel beams with web openings," *Steel Compos. Struct.*, vol. 23, no. 6, pp. 647–656, 2017, doi: 10.12989/scs.2017.23.6.647.
- S. G. Morkhade, M. Kshirsagar, R. Dange, and A. Patil, "Analytical study of effect of web opening on flexural behaviour of hybrid beams," *Asian J. Civ. Eng.*, vol. 20, no. 4, pp. 537–547, 2019, doi: 10.1007/s42107-019-00122-4.
- S. G. Morkhade, R. Dange, M. Kshirsagar, and A. Patil, "Comparative Study of Hybrid and Homogeneous Steel Beams With Web Openings," 2018.
- S. G. Morkhade, S. Shaikh, A. Kumbhar, A. Shaikh, and R. Tiwari, "Comparative study of ultimate load for castellated and plain-webbed beams," *Int. J. Civ. Eng. Technol.*, vol. 9, no. 8, pp. 1466–1476, 2018, Accessed: Jun. 07, 2022. [Online]. Available: [https://www.researchgate.net/profile/Samadhan-Morkhade/publication/328272756\\_Comparative\\_study\\_of\\_ultimate\\_load\\_for\\_castellated\\_and\\_plain-webbed\\_beams/links/60ee860bfb568a7098a9fc2a/Comparative-study-of-ultimate-load-for-castellated-and-plain-webbed-beams](https://www.researchgate.net/profile/Samadhan-Morkhade/publication/328272756_Comparative_study_of_ultimate_load_for_castellated_and_plain-webbed_beams/links/60ee860bfb568a7098a9fc2a/Comparative-study-of-ultimate-load-for-castellated-and-plain-webbed-beams)
- S. R. El-Khoriby, M. F. Hassanein, O. F. Kharoob, A. M. El Hadidy, and G. A. N. Alnaggar, "Tubular flange plate girders with corner square web openings in the panel of maximum shear: Strength and behaviour," *Thin-Walled Struct.*, vol. 99, pp. 142–154, 2016, doi: 10.1016/j.tws.2015.11.014.
- T. C. H. Liu and K. F. Chung, "Steel beams with large web openings of various shapes and sizes: Finite element investigation," *J. Constr. Steel Res.*, vol. 59, no. 9, pp. 1159–1176, 2003, doi: 10.1016/S0143-974X(03)00030-0.
- T. Hoglund, "Strength of thin plate girders with circular or rectangular web holes without web stiffeners," in *Proceedings of the Colloquium of the International Association of Bridge and Structural Engineering*, London, 1971, pp. 353–366.
- V. T. Lian and N. E. Shanmugam, "Openings in horizontally curved plate girder webs," in *Thin-Walled Structures*, 2003, vol. 41, no. 2–3, pp. 245–269. doi: 10.1016/S0263-8231(02)00090-3.
- V. Thevendran and N. E. Shanmugam, "Lateral Buckling of Doubly Symmetric Beams Containing Openings," *J. Eng. Mech.*, vol. 117, no. 7, pp. 1427–1441, 1991, doi: 10.1061/(asce)0733-9399(1991)117:7(1427).
- Y. Ali, M. El-Boghdadi, and A. El Hadidy, "Cyclic shear performance of hollow tubular flange plate girders: a numerical study," 2021.
- Y. O. Özkılıç, "Optimized stiffener detailing for shear links in eccentrically braced frames," *Steel Compos. Struct.*, vol. 39, no. 1, pp. 35–50, 2021, doi: 10.12989/scs.2021.39.1.035.